Inorganic Chemistry

Article

pubs.acs.org/IC

Mn^{III}(tetra-biphenyl-porphyrin)−TCNE Single-Chain Magnet via Suppression of the Interchain Interactions

Ryuta Ishikawa, Keiichi Katoh, Brian K. Breedlove, and Masahiro Yamashita*

Department of Chemistry, Graduate School of Science, Tohoku University, 6-3 Aramaki-Aza-Aoba, Aoba-ku, Sendai, Miyagi 980-8578, Japan

Supporting Information

ABSTRACT: A single-chain magnet (SCM) of [Mn(TBPP)(TCNE)]·4*m*-$PhCl_2$ (**1**), where $TBPP^{2-}$ = *meso*-tetra(4-biphenyl)porphyrinate; $TCNE^{\bullet -}$ = tetracyanoethenide radical anion; *m*-$PhCl_2$ = *meta*-dichlorobenzene, was prepared via suppression of interchain interactions. **1** has a one-dimensional alternating Mn^{III}(porphrin)−$TCNE^{\bullet -}$chain structure similar to those of a family of complexes reported by Miller and co-workers. From a comparison of the static magnetic properties of **1** with other Mn^{III}(porphyrin)−$TCNE^{\bullet -}$ chains, a magneto-structural correlation between the intrachain magnetic exchange and both the dihedral angle between the mean plane on [Mn(TBPP)(TCNE)] and Mn−N≡C was observed. The ac magnetic susceptibility data of **1** could be fit with the Arrhenius law, indicating that slow magnetic relaxation and ruling out three-dimensional long-range ordering and spin-glass-like behavior. The Cole−Cole plot for **1** was semicircular, verifying that it is an SCM. Therefore, **1** is an ideal single-chain magnet with significantly strong intrachain magnetic exchange interactions beyond the Ising limit.

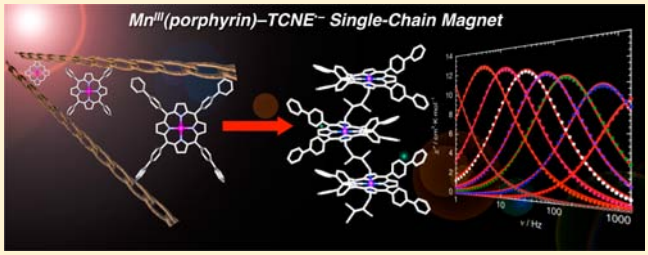

INTRODUCTION

Single-chain magnets (SCMs) are superparamagnet-like isolated one-dimensional (1D) magnetic molecular materials.[1,2] Chemists have developed synthetic strategies to assemble various types of SCMs with predetermined topologies.[3] Over nearly four decades ago, R. J. Glauber first predicted SCMs on the basis of the slow dynamics of the magnetization in ferromagnetic Ising chains.[4] SCMs are not strictly Ising spin chains but can be described by using a finite anisotropic Heisenberg spin chain model.[1,2,3c,5,6,7,8] The slow dynamics of the magnetization of SCMs falling within the Ising limit[6] ($|D/J| \gg 4/3$, where D is the magnetic anisotropy and J is the magnetic exchange interaction) have been studied extensively using a series of ferromagnetic SCMs composed of 2:1 assemblies of Mn^{III}(salen)-type and Ni^{II} oximate complexes[2,7] and Mn^{III}(salen)-type and $[Fe^{III}(CN)_6]^{3-}$ complexes.[8] In the case of these SCMs, the activation energy gap ($\Delta_{\tau i}$) depends on the chain length (L) and the correlation length (ξ). In the high-temperature region (infinite-size regime), when L is larger than ξ, nucleation occurs at two domain edges in the chain. Thus, $\Delta_{\tau 1}$ becomes $2\Delta_\xi + \Delta_A$ (where $\Delta_\xi = 4JS^2$, which indicates the correlation energy needed to create a domain wall, and $\Delta_A = |D|S^2$, which is the anisotropy energy). However, in the low-temperature region (finite-size regime), when L is much shorter than ξ, nucleation occurs on only one side of the domain edge in the chain, and $\Delta_{\tau 2} = \Delta_\xi + \Delta_A$.[2,3c,5,7,8] As noted above, SCMs have a distinct advantage over single-molecule magnets (SMMs), because of an additional energy term known as Δ_ξ involving J between the magnetic spins. This advantage may lead to high relaxation barriers in low-dimensional superparamagnets.

On the other hand, when $|J|$ is much larger than $|D|$, namely less than the Ising limit ($|D/J| \ll 4/3$), the relaxation dynamics are not well understood. For $|D/J| \gg 4/3$, the width of the domain wall is sharp and/or narrow, whereas for $|D/J| \ll 4/3$, the domain wall has a finite thickness, i.e., a "broad domain wall".[9] The mechanism for the slow relaxation of SCMs in this regime needs to be fully elucidated in order to create better SCMs. However, the Glauber model cannot be used in this region and, thus, must be revised for SCMs with a broad domain wall.

Miller and co-workers have reported anisotropic quasi-one-dimensional (quasi-1D) ferrimagnetic chains composed of charge-transfer complexes of Mn^{III}(porphyrin) derivatives (D^+) and organic anion radicals ($A^{\bullet -}$), such as $TCNE^{\bullet -}$[10] and related organic radical anions,[11] $\cdots D^+A^{\bullet -}D^+A^{\bullet -}\cdots$. The magnetic exchange interactions between the Mn^{III} ions and the radical anions are considerably strong.[10,11] In addition, the ac susceptibility of some of these systems is dependent on the frequency, which is indicative of a slow relaxation process. In other words, Mn^{III}(porphyrin) derivatives are good models for SCMs beyond the Ising limit. However, Epstein and co-workers have suggested that viscous magnetic behavior is caused by disorder, leading to quasi-1D clusters coupled through dipole−dipole interactions between chains to form 3D domains.[10,11]

Received: July 14, 2012
Published: August 1, 2012

dx.doi.org/10.1021/ic3015223 | *Inorg. Chem.* 2012, 51, 9123−9131

Moreover, the crystal lattices of most Mn^{III}(porphyrin) derivatives contain interstitial solvent molecules, which affect their magnetic behaviors due to absorption/desorption processes, known as magnetic sponge effects.[10l,u,z] Bałanda and co-workers have reported that [Mn(T*o*-FPP)-(TCNE)]·2PhMe has peculiar magnetic properties, such as SCM-like behavior. It has clearly been shown that the magnetism in the family of Mn^{III}(porphyrin)−$TCNE^{\bullet -}$ chains can be tuned by the nature of substituents on the porphyrin ligand. As mentioned above, however, it is difficult to determine whether they are spin glasses (SGs) or superparamagnets.

For the elucidation of the slow relaxation mechanism of SCMs beyond the Ising limit, it is necessary to prepare an Mn^{III}(porphyrin)−$TCNE^{\bullet -}$ SCM. In order to prepare an Mn^{III}(porphyrin)−$TCNE^{\bullet -}$ SCM, the following were key factors: (i) suppression of the interchain interactions, including through-space magnetic interactions, and (ii) a highly stabilized crystal packing. The magnetic behavior of Mn^{III}(porphyrin)−radical derivatives can be tuned by changing the substituents on the porphyrin rings and changing the interstitial solvent molecules. In other words, SCMs can be prepared by controlling the chain structure and its crystal packing. Herein, we report a new Mn^{III}(porphyrin)−$TCNE^{\bullet -}$ chain that behaves experimentally as an SCM with a slow relaxation mechanism beyond the Ising limit. [Mn(TBPP)(TCNE)]·4*m*-$PhCl_2$ (**1**) is composed of a Mn^{III}(porphyrin) unit with bulky biphenyl groups on the *meso* positions of the porphyrin ring, which act as good chain separators, preventing interchain magnetic interactions, and $TCNE^{\bullet -}$. **1** has a ferrimagnetic alternating chain topology similar to those of Miller's compounds.

EXPERIMENTAL SECTION

Synthetic Materials and Methods. Reagents and solvents were purchased from Tokyo Kasei Co. Ltd. and Wako Pure Chemical Industries Ltd. Reagents were reagent grade and used without further purification. Solvents were distilled before use under a N_2 atmosphere, using the appropriate drying agents. All procedures were carried out under a N_2 atmosphere using Schlenk techniques or in a N_2 atmosphere glovebox.

Physical Measurements. Elemental analyses (E.A.) and Fourier transform mass spectrometry (FT-MS) were performed on a Micro Corder JM10 (J-Science Lab Co., Ltd.) and an APEX III FT-MS system (Bruker Daltonics, Inc.), respectively, by the Technical Support Division, Research and Analytical Center for Giant Molecules, Graduate School of Science, Tohoku University. Infrared (IR) spectra were acquired as KBr disks at room temperature on a Jasco Model FT-IR 620 spectrophotometer. Differential thermal gravimetric (DTG) analysis (293−823 K) was carried out with a Shimadzu Model DTG-60H instrument in a N_2 atmosphere (heating rate: 10 K min^{-1}). Magnetic data were collected on a Quantum Design MPMS-XL SQUID magnetometer (Quantum Design, Inc.). Measurements for all compounds were obtained using finely ground microcrystalline powders restrained by Nujol or eicosane in a polycarbonate capsule. dc susceptibility measurements were collected in the temperature range of 1.8−300 K in a dc field of 0.1 T. Field-dependent dc magnetization measurements were performed from −7 T to 7 T in a temperature range of 1.8−6.0 K. ac susceptibility measurements were performed in the temperature range of 1.8−100 K in a 3 Oe ac field oscillating at frequencies of 1 and 1488 Hz with no applied dc field. Magnetic susceptibility data were corrected for diamagnetic contributions from the sample holder as well as for the core diamagnetism of each sample estimated using Pascal's constants.[13] Because the commonly used units of experimentally and theoretically estimated parameters are Kelvin (K), all values in this manuscript are divided by the Boltzmann constant.

Synthesis of *meso*-tetra(4-biphenyl)porphyrin (H_2TBPP). The free-base porphyrin was synthesized using a slightly modified literature method.[12] To a solution of 4-phenylbenzaldehyde (0.91 g, 5 mmol) in $CHCl_3$ (500 mL) was added pyrrole (0.356 mL, 5 mmol), followed by dropwise addition of BF_3·Et_2O (6 μL, 5×10^{-2} mmol). The mixture was stirred for 2.5 h at room temperature, during which the color of the solution changed from colorless to dark red. DDQ (0.10 mg, 4 mmol) then was added, and the mixture was refluxed for an additional 4 h. The solvent was removed, and the residue was subjected to chromatography on a silica gel column. After a yellow fraction containing unreacted DDQ was eluted with CH_2Cl_2/hexane (1:1), a second red-purple fraction corresponding to H_2TBPP was eluted with $CHCl_3$. The solvent was removed under reduced pressure, affording a purple crystalline solid. Yield: 540 mg (12%). FT-MS (*m*/*z*): $[M + H]^+$ Calcd for $C_{68}H_{46}N_4$, 919.3801; Found, 919.3792.

Synthesis of [Mn(TBPP)Cl]. $Mn(OAc)_2$·$4H_2O$ (2 g, 8.2 mmol) was added to a solution of H_2TBPP (0.75 g, 0.82 mmol) in DMF (450 mL). The solution was then refluxed for 10 h. The reaction was monitored using thin-layer chromatography (TLC), and reflux was stopped when no H_2TBPP remained. After cooling, the reaction mixture was poured into distilled water (2 L). The resulting green precipitate was collected on Celite and washed with water. After drying, it was then dissolved in $CHCl_3$ (300 mL), and the solution poured into an equal volume of an aqueous 6 M HCl solution. The mixture was stirred vigorously for 12 h. The organic phase was collected and dried over anhydrous $MgSO_4$, and then the solvent was removed under reduced pressure. The residue was subjected to chromatography on a silica gel column. After a deep-red fraction containing freebase H_2TBPP was eluted with AcOEt/$CHCl_3$ (3:1), a green fraction containing [Mn(TBPP)-Cl] was eluted with $CHCl_3$. The solvent was removed under reduced pressure, affording a deep-green crystalline solid, [Mn(TBPP)Cl]. Yield: 0.64 g (77%). Dark-green single crystals of [Mn(TBPP)Cl]·$CHCl_3$·$0.75H_2O$ suitable for single-crystal X-ray diffraction (XRD) were obtained from $CHCl_3$/hexane. Crystallographic and magnetic data were obtained with the crystals in contact with the mother liquor to prevent solvent loss. Elemental analysis was performed on a vacuum-dried sample. The dried sample was hygroscopic. Anal. Calcd. for $C_{68}H_{46}ClMnN_4O$: C, 79.64; H, 4.52; N, 5.46%. Found: C, 80.12; H, 4.18; N, 5.54%. FT-MS (*m*/*z*): $[M]^+$ calcd. for $C_{68}H_{46}N_4$, 971.2946; Found, 971.2936.

Synthesis of [Mn(TBPP)(Py)]. To a solution of [Mn-(TBPP)Cl] (0.72 g, 0.71 mmol) in pyridine (60 mL) and MeOH (20 mL) was added $NaBH_4$ (0.61 g, 16 mmol), and then the mixture was refluxed for 30 min. After cooling, 60 mL of degassed MeOH was added to the reaction mixture. The precipitate was collected, washed three times with a small amount of MeOH, and dried to yield [Mn(TBPP)(Py)] as a blue-green crystalline solid. Yield: 687 mg (92%). The product was used for the next reaction without further purification.

Synthesis of [Mn(TBPP)(TCNE)]·4*m*-$PhCl_2$ (1). A *m*-$PhCl_2$ solution (1 mL) of [Mn(TBPP)(Py)] (75.3 mg, 0.07 mmol) was transferred to a glass tube, and then a solution of

dx.doi.org/10.1021/ic3015223 | *Inorg. Chem.* 2012, 51, 9123−9131

TCNE (35.5 mg, 0.28 mmol) in *m*-$PhCl_2$ (1 mL) was layered onto the first solution without mixing while in a glovebox. Black crystals formed at ambient temperature after several days. Yield: 37.5 mg (31%). Anal. Calcd. for $C_{98}H_{60}Cl_8MnN_8$: C, 69.39; H, 4.04; N, 6.61%. Found: C, 69.41; H, 4.20; N, 6.72%. IR (KBr, cm^{-1}): ν_{CN} = 2190−2213 cm^{-1} (br), 2129 cm^{-1} (s), 2143 cm^{-1} (s).

General Methods for X-ray Crystallography. Air-sensitive samples were coated with Nujol or Paratone-N oil (Hampton Research Corp.) while in the mother liquid and mounted quickly to avoid decomposition. Crystals of both compounds were mounted on MicroLoops (MiTeGen, Inc.) and immediately cooled in a N_2 cold stream. Data collection was performed on a Rigaku CCD diffractometer (Saturn70) with graphite-monochromated Mo Kα radiation (λ = 0.71070 Å) and a low-temperature apparatus. The crystal dimensions were 0.70 mm × 0.30 mm × 0.20 mm for [Mn(TBPP)Cl] and 0.18 mm × 0.08 mm × 0.07 mm for **1**. The data for [Mn(TBPP)Cl] were collected at 93(1) K, and those for **1** were collected at 103(1) K. Data integration, preliminary data analysis, and absorption correction were performed using the Rigaku CrystalStructure crystallographic software package.[14] The structure was solved using direct methods with SIR97[15] and refined using the SHELXL program.[16] All non-hydrogen atoms were refined anisotropically, except for some disordered atoms that were refined isotropically. All hydrogen atoms were introduced as fixed contributors. The Cl atom coordinated to the Mn^{III} ion in [Mn(TBPP)Cl] was disordered with an occupancy factor of 0.75 for Cl(1) and 0.25 for Cl(2). The $TCNE^{\bullet -}$ moieties had two locations in **1** with the minor form being rotated 90° with respect to major form and in the same plane as the major form (major:minor = 7:3). CCDC-876962-876963, representing [Mn(TBPP)Cl] and **1**, contain the supplementary crystallographic data for this paper. These data can be obtained free of charge from The Cambridge Crystallographic Data Centre via www.ccdc.cam.ac.uk/data_request/cif. The crystal data and details of the structure determination of the compound of **1** are summarized in Tables 1 and 2.

RESULTS AND DISCUSSION

Synthesis, Structure, and Magnetic Properties of [Mn(TBPP)Cl]. The Mn^{III}(porphyrin) precursor used to prepare the Mn^{III}(porphrin)−$TCNE^{\bullet -}$ chain was synthesized using a typical procedure: (i) the free base porphyrin (H_2TBPP) was isolated, and (ii) and then it was coordinated to the Mn^{III} ions, affording [Mn(TBPP)Cl]. Each reaction was performed using previously reported procedures.[17]

[Mn(TBPP)Cl] crystallized in the monoclinic space group $P2_1/n$ (see Figure S1 in the Supporting Information). The average Mn−N coordination distance is 2.006 Å, and the Mn^{III} ion is 0.175 Å above the plane formed by the four N atoms of the $TBPP^{2-}$ ligand. The apical Mn(1)−Cl(1) bond distance is 2.411(2) Å. The geometry around the Mn^{III} atom is a slightly distorted square pyramid involving the four N atoms of the $TBPP^{2-}$ ligand and the axially coordinated Cl atom with a trigonal distortion parameter (τ) of 0.023.[18] [Mn(TBPP)Cl] molecules are arranged in a two-dimensional square-grid array with no intermolecular contacts. H_2O and $CHCl_3$ were found in the void spaces between four [Mn(TBPP)Cl] molecules with the disordered axial Cl atom hydrogen-bonded with the interstitial H_2O molecules. The nearest neighbor intermolecular Mn···Mn distance between layers was determined to be 12.540 Å. Consequently, [Mn(TBPP)Cl] is a good building unit to prepare well-isolated chain complexes because of the steric repulsion between the bulky biphenyl substituents at the *meso*-positions of the $TBPP^{2-}$ ligand.

Table 1. Crystallographic Data for 1

parameter	value/comment
compound	**1**
formula	$C_{98}H_{60}Cl_8MnN_8$
formula weight	1688.17
crystal system	monoclinic
space group	$P2_1/a$ (#14)
lattice parameters	
a	17.014(2) Å
b	22.785(3) Å
c	20.890(3) Å
β	101.3048(18)°
V	7941.1(18) $Å^3$
Z	4
D_{calc}	1.412
F_{000}	3460.00
μ(Mo Kα)	4.914 cm^{-1}
No. of reflections measured	total: 52970 (R_{int} = 0.036)
No. observations (all reflections)	13899
No. variables	1081
R (all reflections)	0.0818
R_1 ($I > 2.00\sigma(I)$)[a]	0.0669
wR_2 (all reflections)[b]	0.1870
goodness of fit, GOF	1.075

[a] $R_1 = \sum||F_0| - |F_c||/\sum|F_0|$ ($I > 2.00\sigma(I)$). [b] $wR_2 = [\sum w(F_0^2 - F_c^2)^2]/\Sigma w(F_0^2)^2]^{1/2}$ (All reflections).

The temperature dependence of the dc magnetic susceptibility data was studied with a fresh polycrystalline sample of [Mn(TBPP)Cl] in the temperature range of 1.8−300 K in a 0.1 T dc field (see Figure S2 in the Supporting Information). The χT value was determined to be 2.8 cm^3 K mol^{-1} at 300 K, which corresponds to the spin-only value of a high-spin Mn^{III} ion (S_{Mn} = 2) ground state with g_{Mn} < 2.0. It remained constant to ∼30 K, and then abruptly decreased. This behavior suggests that appreciable zero-field-splitting (ZFS) causes the S = 2 ground state, which is typical for other high-spin Mn^{III}-porphyrin derivatives.[19] The magnetic behavior was fit with an isolated S_{Mn} = 2 ground state and the ZFS term D_{Mn}, taking into account the temperature-independent paramagnetism (TIP), using the following spin Hamiltonian:

$$\mathcal{H}_{ZFS} = D_{Mn}\left[S_z^2 - \frac{S(S+1)}{3}\right] + g_{Mn}\mu_B S_{Mn} H$$

where μ_B and k_B are Bohr magneton and Boltzmann constant, respectively. The obtained best-fit parameters were determined to be g_{Mn} = 1.95, and D_{Mn}/k_B = −3.8 K (= −2.7 cm^{-1}). The D value falls within the range between −1.6 K and −5.5 K (−1.1 cm^{-1} to 3.8 cm^{-1}) reported for related five-coordinate and six-coordinate high-spin Mn^{III}(porphyrin) derivatives.[19]

SYNTHESIS, STRUCTURE, AND CHARACTERIZATION OF 1

A new Mn^{III}(porphyrin)−$TCNE^{\bullet -}$ chain was synthesized by reacting[20] the reduced form of [Mn(TBPP)Cl] ([Mn(TBPP)(Py)], where Py = pyridine) with neutral TCNE. In the IR spectrum of **1**, bands observed at 2129, 2143, and 2190−2213

dx.doi.org/10.1021/ic3015223 | Inorg. Chem. 2012, 51, 9123−9131

Table 2. Bond Lengths, Angles, and Parameters for 1D Mn^{III}(porphyrin)−$TCNE^{\bullet -}$ Chain Complexes Including 1

compound	Mn−N [Å]	∠Mn−N≡C [deg]	dihedral angle [deg][b]	intrachain Mn···Mn [Å][c]	θ' [K][d]	T_{min} [K][e]	J/k_B [K][f]	J/hc [cm^{-1}][f]	ref
[Mn(TBrPP)(TCNE)]·2PhMe (a)	2.293	168.1	89.4	10.277	+13	80	−30	−21	10p, q
[Mn(TClPP)(TCNE)]·2PhMe (b)	2.267	167.2	86.8	10.189	+13	110	−33	−23	10l, m, o, q, z
[Mn(TOMePP)(TCNE)]·2PhMe (c)	2.289	165.5	78.1	10.256	+21	134			10k, m
[Mn(TIPP)(TCNE)]·2PhMe (d)	2.276	158.7	69.6	10.101	+30	160	−53	−37	10q
[Mn(TPP)(TCNE)]·2PhMe (e)	2.305 (av)	147.9 (av)	55.4 (av)	10.116	+44	191	−63	−44	10f, m, u
[Mn(To-FPP)(TCNE)]·2PhMe (f)[a]	2.313 (av)	148.6 (av)	55.4 (av)	10.185	+45	240	−109	−75	9a, 10k, 28
[Mn(TP′P)(TCNE)]·2PhMe (g)	2.299	129	30.4	8.587	+90	>300			10f, m
[Mn(TBPP)(TCNE)]·4*m*-$PhCl_2$ (1)	2.320 (av)	125.2 (av)	27.9 (av)	9.417	+91	>300	−122	−84	this work

[a]The substituent is located at the *meso* position of the porphyrin ring for all compounds, which is located at the *para* position, whereas that of only (f) is the *ortho* position. [b]The angle is defined by the dihedral angle involving $TCNE^{\bullet -}$ and the Mn^{III}(porphyrin) planes. [c]This distance is through the bridging *trans*-μ_2-*N*-coordinated $TCNE^{\bullet -}$. [d]Effective θ' value (see text). [e]Temperature at which the minimum value of χT occurs. [f]Fitted by using the Seiden expression (see text). All Mn^{III}(porphrin)−$TCNE^{\bullet -}$ chain compounds, except for **1**, were reported by Miller and co-workers,[10] and the *J* value for f was reported by Tomkowicz and co-workers.

cm^{-1} are typical for CN stretching modes of *trans*-μ_2-*N*-coordinated radical anion form of TCNE (Figure 1).[21] These

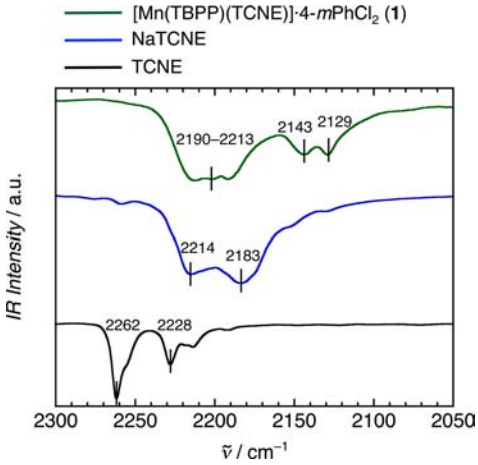

Figure 1. IR spectra of TCNE, NaTCNE, and **1**.

results are consistent with the crystallographic and magnetic studies (vide infra). DTG analysis of **1** showed the loss of the crystallization solvent molecules in the temperature range of 70−165 °C (see Figure S3 in the Supporting Information). The number of solvent molecules are consistent with that determined from single-crystal analysis (vide infra).

Complex **1** crystallized in the monoclinic space group $P2_1/a$. Figure 2 shows an ORTEP drawing and the chain motif of **1**. The structure is an alternating zigzag chain composed of $[Mn(TBPP)]^+$ (D^+) and $TCNE^{\bullet -}$ ($A^{\bullet -}$), i.e., $\cdots D^+A^{\bullet -}D^+A^{\bullet -}\cdots$, with four *m*-$PhCl_2$ molecules in the crystal lattice. The geometry around the Mn^{III} ion is distorted octahedral involving the four N atoms of $TBPP^{2-}$ and two N atoms of the bridging $TCNE^{\bullet -}$ moiety in a *trans*-μ_2-*N*-coordination mode. The average equatorial Mn−N coordination distance is 2.005 Å, which is similar to that of [Mn(TBPP)Cl]. On the other hand, the average axial Mn−N bond distances (2.320 Å) are much longer than the equatorial ones due to Jahn−Teller distortion. The $[Mn(TBPP)]^+$ unit is significantly distorted from planarity. The ruffling of the $[Mn(TBPP)]^+$ unit is superimposed on a saddle deformation, resulting in a decrease in the overall symmetry. As seen with other ruffled $[Mn(TBPP)]^+$ units, the biphenyl groups at the *meso*-position alternate up and down in relation to the $[Mn(TBPP)]^+$ plane. The averaged dihedral angle between the opposing pyrrole planes was determined to be 18.66°, which is due to the steric repulsion between the bulky *meso*-biphenyl substituents. The dihedral angle between the mean planes of $[Mn(TBPP)]^+$ and $TCNE^{\bullet -}$ was determined to be 27.86°. The averaged Mn^{III}−N≡C angle is 125.18°. The nearest neighbor and second nearest-neighbor intrachain Mn···Mn separations through the $TCNE^{\bullet -}$ bridge were 9.417 Å and 17.014 Å, respectively. The crystal packing arrangement of the chains of **1** is shown in Figure 3.

The chains run parallel to the crystallographic *a*-axis. The nearest interchain Mn···Mn separation between *in-registry* chains was 12.637 Å, whereas that between *out-of-registry* chains was 20.890 Å. The chains aggregate together to form 1D channel-like structures, in which *m*-$PhCl_2$ molecules are tightly captured. However, no significant intermolecular interactions, such as hydrogen bonding and stacking interactions, were observed between the chains, as well as between the chains and the interstitial solvent molecules.

Static Magnetic Properties of 1. Static dc magnetic measurements were performed on selected ground crystals of **1** in the temperature range of 1.8−300 K in a 0.1 T field (Figure 4).

The χT value of **1** at 300 K was 2.7 cm^3 K mol^{-1}, which is smaller than the theoretical value (3.4 cm^3 K mol^{-1} with g_{Mn} = 2.0, g_{Rad} = 2.0) based on an isolated high-spin Mn^{III} ion (S_{Mn} = 2) and a mono radical anion $TCNE^{\bullet -}$ (s_{Rad} = 1/2). The values increased gradually with a decrease in the temperature, reaching a maximum value of 80.2 cm^3 K mol^{-1} at 16 K. Below 16 K, χT abruptly decreased to 11.6 cm^3 K mol^{-1} at 1.8 K. This behavior is indicative of strong antiferromagnetic coupling between the Mn^{III} ions (S_{Mn} = 2) and $TCNE^{\bullet -}$ (s_{Rad} = 1/2) within the chains. Miller and co-workers fit the magnetic behavior of their Mn^{III}(porphyrin)−TCNE chains using the Seiden model[22] of

dx.doi.org/10.1021/ic3015223 | Inorg. Chem. 2012, 51, 9123−9131

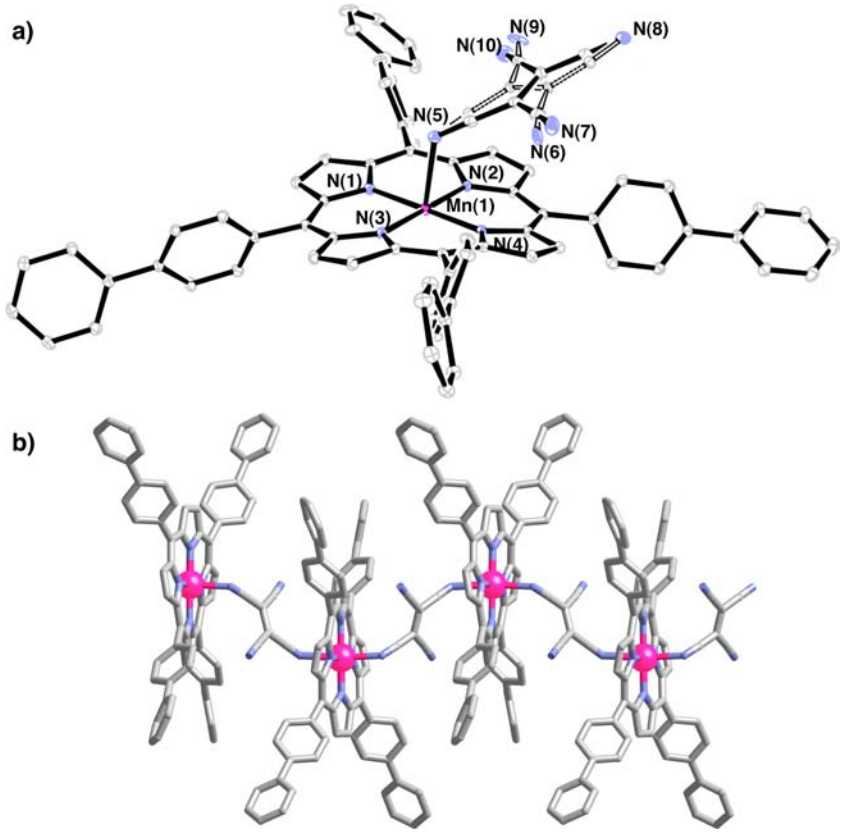

Figure 2. (a) ORTEP drawing with 30% probability thermal ellipsoids of the single-crystal X-ray crystal structure and (b) chain motif of **1**. Hydrogen atoms and interstitial solvent molecule are omitted for the sake of clarity.

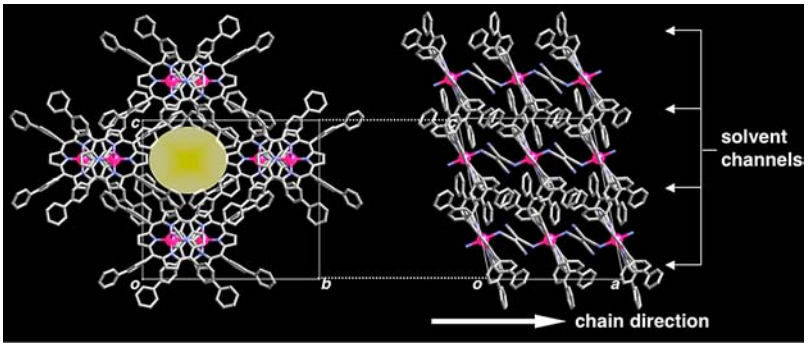

Figure 3. Representation of four adjacent chains in the crystal packing of **1**. (a) Top and (b) side views of the chain. Light-yellow sphere indicates the 1D channel formed by four adjacent chains. Interstitial *m*-$PhCl_2$ molecules and hydrogen atoms are omitted for the sake of clarity.

alternating chains of classical spins (S_i) and quantum spins (s_i), using the following spin Hamiltonian:

$$\mathcal{H} = -2J \sum_{i=1}^{N} (S_{\mathrm{Mn},i} + S_{\mathrm{Mn},i+1}) \cdot S_{\mathrm{Rad},i}$$

By fitting the data above 30 K, the value of J/k_B was determined to be −136.1 K (−94.5 cm^{-1}) using g_{Mn} = 2.0 and g_{Rad} = 2.0, indicating the existence of strong antiferromagnetic coupling between neighboring magnetic centers. However, minimum values of T (T_{min}) and the Weiss constant (θ) were not observed in the χT plot for **1**, which must be acquired at a higher temperature. Above 150 K, the magnetic susceptibility could be fit using the Curie−Weiss expression with an effective θ' value of +90.9 K (see Figure 4).

For classical 1D systems, $\chi'T$, where χ' is the in-phase zero field susceptibility, is related to the correlation length (ξ) in a zero dc field when the anisotropic Heisenberg or Ising-like 1D system behaves exponentially:

$$\chi'T \approx C_{\mathrm{eff}} \exp\left(\frac{\Delta_\xi}{k_B T}\right)$$

where C_{eff} and Δ_ξ are the effective Curie constant and the correlation energy, respectively.[23] On the basis of this relationship, the temperature dependence of ac magnetic susceptibility was studied in an oscillating magnetic field of 3 Oe with a frequency of 1 Hz and a zero dc field. The $\chi'T$ products increased linearly as the temperature decreased, reaching a maximum value ($[\chi'T]_{max}$) of 279 cm^3 K mol^{-1} at ca. 11.5 K. It remained constant to ca. 8.5 K, and then abruptly

dx.doi.org/10.1021/ic3015223 | *Inorg. Chem.* 2012, 51, 9123−9131

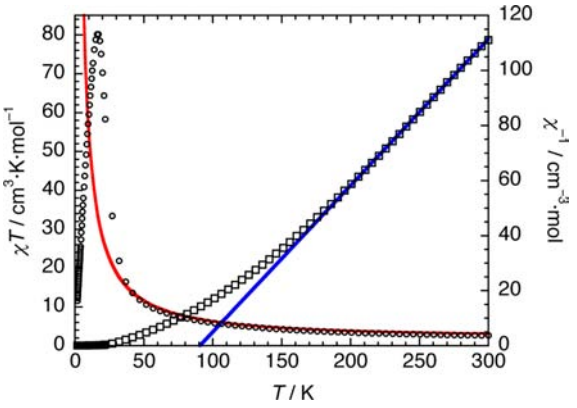

Figure 4. Temperature dependence of (○) χT and (□) $1/\chi$ of **1**. The red and blue solid lines represent best-fit curves. The fitting model is described in the text.

decreased until χ' is blocked at a frequency of 1 Hz. The plot of $\chi'T$ versus $1/T$ was linear in the temperature range of 18−60 K (Figure 5). From the slope of the line, C_{eff} = 2.7 cm^3 K mol^{-1}

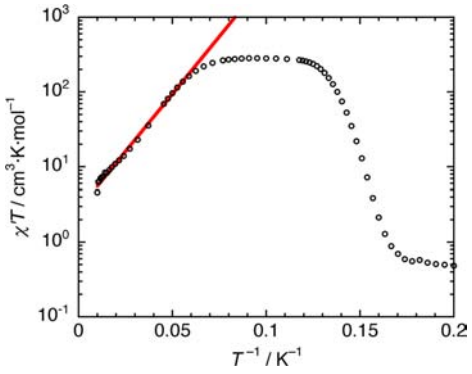

Figure 5. Plot of $\chi'T$ with a semilogarithmic scale versus $1/T$ for **1** in the temperature range of 5.0−100 K.

and Δ_ξ/k_B = 70.8 K (49.2 cm^{-1}), which corresponds to the energy required to create a domain wall within the chain. For 1D systems falling within the Ising limit, Δ_ξ^{Ising} is related to the magnitude of J and constituent spins through the expression $\Delta_\xi^{Ising} = 4|J|S_{Mn}S_{Rad}$.[5d] For **1**, considering the J value, Δ_ξ^{Ising}/k_B = 544 K (377 cm^{-1}), which is much larger than the experimental value. This disagreement clearly shows that **1** does not have sharp domain walls. In other words, for **1**, $|J|$ is much larger than $|D|$. Below 12 K, the $\chi'T$ product shows the $[\chi'T]_{max}$ value, as expected in the presence of finite-size effects when $\xi \gg L$. The estimated chain lengths of ca. 100 nm based on $[\chi'T]_{max}/C_{eff}$ is rather small.[5d]

The field dependence of the magnetization for **1** was measured in the temperature range of 1.8−6 K (see Figure 6). Below 6 K, slow relaxation of the magnetization was observed. The coercivity increased with a decrease in the temperature. The coercive field was 2.7 T at 1.8 K. As seen in the plot of M versus H for 1 at 1.8 K, the magnitude of the magnetization at 7 T (2.2 μ_B) is smaller than the expected value (3 μ_B, $S_T = 2 - 1/2 = 3/2$), indicating the presence of significant magnetic anisotropy within the chains. Extrapolation of the linear part of the magnetization curve on the higher field side to its intersection with the expected magnetization value gives the magnetization at saturation (H_a), which was estimated to be

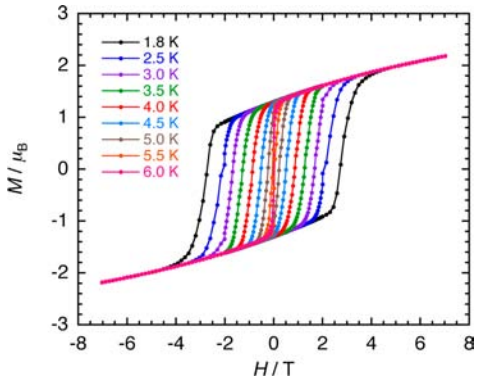

Figure 6. Field dependence of magnetization curves for **1**, collected from 1.8 to 6.0 K. The solid lines serve as guides for the eye.

~14.7 T from Figure S4 in the Supporting Information. Thus, D_{Mn} can be estimated via the following expression:

$$-2D_{Mn}S_{Mn}^2 = g\mu_B S_T H_a$$

where S_T = 3/2. D_{Mn}/k_B was estimated to be −3.7 K (−2.6 cm^{-1}), which agrees with that for [Mn(TBPP)Cl] (vide supra).

Magnetostructural Correlations between 1 and Related Compounds. Magnetic exchange in the family of Mn^{III}(porphyrin)−TCNE$^{\bullet-}$ chains occurs through the TCNE$^{\bullet-}$ *trans*-μ_2-*N* coordination bonds. Miller and co-workers have proposed that there are clear magnetostructural correlations involving the intrachain magnetic exchange coupling and either the dihedral angle between the mean planes on Mn^{III}(porphyrin)−TCNE$^{\bullet-}$ or the Mn^{III}−N≡C angle.[10] For comparison, the reported J values, which were calculated using the Seiden expression for 1D chains of S_{Mn} = 2 and s_{Rad} = 1/2 are plotted in Figure 7 and Figures S4 and S5 in

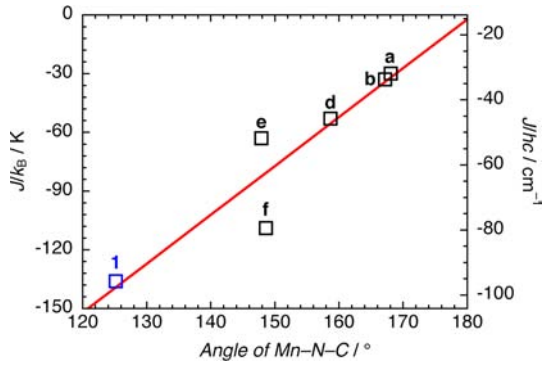

Figure 7. Correlation between the Mn^{III}−N≡C angle defined on Mn^{III}(porphyrin)−TCNE$^{\bullet-}$ and J obtained using the Seiden expression. Labels a−f, and label "1", are explained in Table 2.

the Supporting Information versus Mn^{III}−N≡C angle. The values of J decreased linearly with an increase in the Mn^{III}−N≡C angle (see Figure 7 and Table 2). In other words, the strength of the intrachain magnetic interactions between Mn^{III} and TCNE$^{\bullet-}$ are stronger.

Dynamic Magnetic Properties of 1. The temperature dependence of the ac susceptibilities was measured in the frequency range of 1−1500 Hz in an oscillating ac magnetic field of 3 Oe and a zero dc field (see Figure 8). Below 16 K, in-phase (χ') and out-of-phase (χ'') signals were strongly dependent on the frequency. If the blocking temperature

dx.doi.org/10.1021/ic3015223 | Inorg. Chem. 2012, 51, 9123−9131

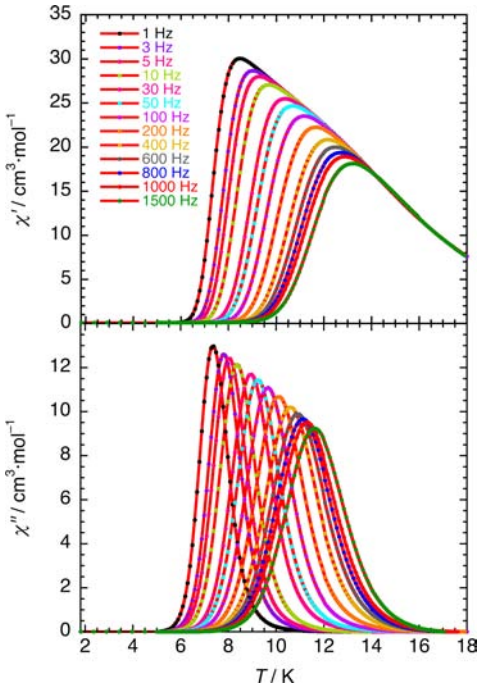

Figure 8. Temperature dependence of the ac susceptibilities (χ' and χ'') of **1** in the frequency range of 1−1500 Hz. The solid lines serve as guides to the eye.

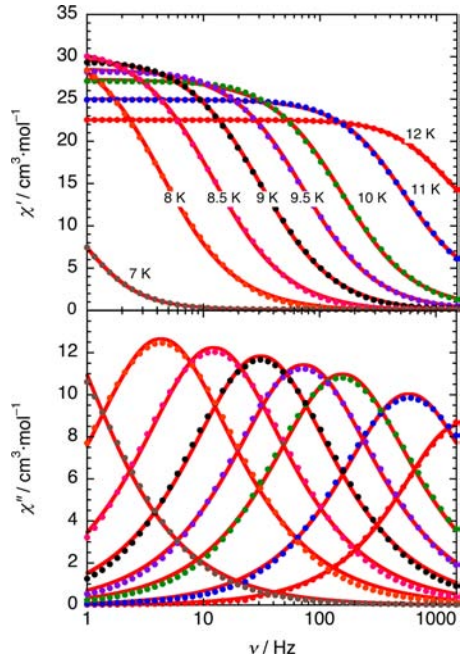

Figure 9. Frequency dependence of ac susceptibilities (χ' and χ'') of **1** collected in the temperature range of 7−12 K. The solid lines are best-fit lines, as described in the text.

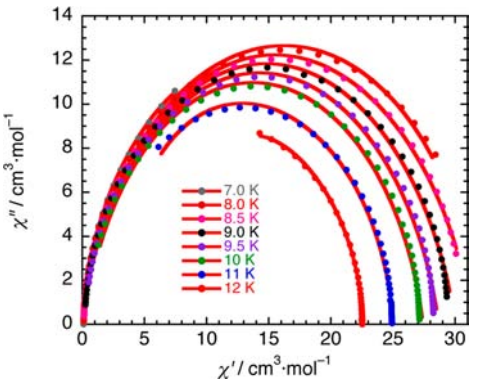

Figure 10. Cole−Cole plots for **1** in the temperature range of 7−12 K. The solid lines were fitted as described in the text.

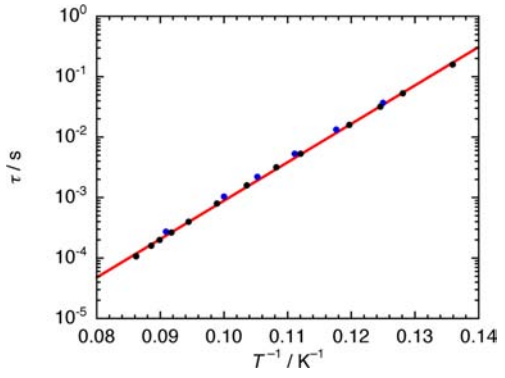

Figure 11. Arrhenius plot of the relaxation time τ for **1** determined from variable temperature (black) and the variable frequency (blue) ac susceptibilities. The solid lines are best-fit lines, as described in the text.

($T_B(\nu)$), which is defined as the temperature below which the relaxation of the magnetization becomes slow, is the temperature where the maximum χ'' value occurs and ν is the frequency of the ac field, the frequency dependence of T_B is given by $\varphi = \Delta T_B/[T_B\Delta(\log \nu)]$.[24] In the case of **1**, the value of φ was determined to be 0.18, which is much greater than those of traditional SGs (0.004−0.08),[24] indicating superparamagnet-like behavior, like SMMs or SCMs, rather than SG behavior.

The magnetization dynamics occur because the chains of **1** are structurally well-isolated and because of the 1D chain magnetism. From the χ'' signals, the relaxation times (τ) were determined using $\tau = 1/(2\pi\nu)$. In addition, ac susceptibility measurements as a function of ν were performed in the temperature range of 7−12 K (see Figure 9).

The obtained data were simulated using a generalized Debye model.[25] Cole−Cole diagrams clearly showed that only one relaxation process occurred since the quasi-semicircle shape could be fitted using the generalized Debye model with α value of 0.04−0.16, as shown in Figure 10.

For SCMs, the resulting relaxation times obey the Arrhenius law ($\tau = \tau_0 \exp(\Delta_\tau/k_BT)$) (see Figure 11).[1,2] From the data, the relaxation barrier (Δ_τ/k_B) was determined to be 146.3 K (101.6 cm^{-1}), with $\tau_0 = 4.1 \times 10^{-10}$ s, the value of which falls within the range typically observed for SCMs.[3] In other words, **1** has a single-relaxation time and does not behave as a spin glass. Moreover, no crossover is observed in the temperature range experimentally available.

Discussion of the SCM properties. As mentioned earlier, the domain wall of SCMs with a large J value has a finite thickness (i.e., broad domain wall).[9] Recently, Billoni and co-workers have theoretically studied the mechanism for the slow magnetic relaxation of SCMs in such a regime, using transfer matrix calculations and time-quantified Monte Carlo simulations on molecular ferromagnetic 1D chains.[9c] According to this theory, the domain wall energy is described by $\Delta_\xi^{Heisenberg} = 2(2|D_{Mn}J|S_{Mn}^3S_{Rad})^{1/2}$ in the broad domain wall regime ($|D| \ll |J|$).[9c,26] On the basis of this considerations, $\Delta_\xi^{Heisenberg}/k_B$ was

dx.doi.org/10.1021/ic3015223 | Inorg. Chem. 2012, 51, 9123−9131

estimated to be 126.9 K for **1**, whereas the experimental value (Δ_ξ/k_B) is 70.8 K, the value of which is more than half of $\Delta_\xi^{Heisenberg}/k_B$. One the other hand, the values of Δ_A unfortunately, there is no perfectly analytical expression using local magnetic parameters (J, D_{Mn}, S_{Mn} and s_{Rad}) in SCMs with the broad domain wall as well as the intermediate regime between the Ising and Heisenberg limits.[3p] Nevertheless, the relationship between $\Delta_{\tau 1} = 2\Delta_\xi + \Delta_A$ and $\Delta_{\tau 2} = \Delta_\xi + \Delta_A$ remains operative for any SCM systems in infinite- and finite-size regimes, respectively. Thus, the value of Δ_A can be estimated from the simple difference of $\Delta_A = \Delta_{\tau 2} - \Delta_\xi$, assuming that the finite-size regime in **1**. The estimated value of Δ_A/k_B are 75.5 K, the value of which is much larger than $\Delta_A/k_B = |D_{Mn}|S_{Mn}^2 = 14.8$ K (10.3 cm^{-1}) for the Ising limit situation, whereas considering the previously obtained $\Delta_\xi^{Heisenberg}$ value of 126.9 K calculated from $\Delta_\xi^{Heisenberg} = 2(2|D_{Mn}J|S_{Mn}^3S_{Rad})^{1/2}$, the anisotropy energy of **1** can be estimated at $\Delta_A/k_B = 19.4$ K (13.5 cm^{-1}), the value of which is comparable to $\Delta_A/k_B = |D_{Mn}|S_{Mn}^2$. This result confirms that the value of Δ_A or the relation of $\chi'T \approx C_{eff}\exp((\Delta\xi)/k_BT)$ for non-Ising ferrimagnetic SCMs with the broad domain wall should become a more-complicated function using local magnetic parameters.

Currently, efforts are underway to prepare SCMs with strong intrachain exchange. Although subsequent investigations on magnetic 1D chain compounds with broad domain walls have been previously reported, only two examples experimentally show ideal SCM characteristics: [Mn(5-TMAMsaltmen)(TCNQ)](ClO$_4$)$_2$[27] and [Mn(T*o*-FPP)(TCNE)].[9a,28] However, further theoretical and experimental studies are necessary. Therefore, in order to deeply understand non-Ising type SCMs, it is important that (i) a general theory ferrimagnetic 1D chains consisting with the isotropic quantum $S = 1/2$ and anisotropic classical $S = 2$ spins via the strong intrachain antiferromagnetic interactions[9c] and (ii) better models and candidates for SCMs beyond the Ising limit are needing.

CONCLUSION

Single-chain magnets (SCMs) can be prepared by controlling the structure and crystal packing of one-dimensional (1D) Mn^{III}(porphyrin)−TCNE$^{\bullet -}$-chain complexes. The magnetic behavior of 1D Mn^{III}(porphyrin)−TCNE$^{\bullet -}$ chain materials (spin glass (SG), 3D magnet, and SCM) depends on the substituent on the porphyrin ring. Specifically, **1** with bulky biphenyl groups, of which the dihedral angle between the mean planes of Mn^{III}(porphyrin)−TCNE$^{\bullet -}$ and Mn^{III}−N≡C were 125.2° and 27.9°, respectively, was synthesized. On the basis of the dc susceptibility data for **1** ($J/k_B = -136$ K and $\theta' = +91$ K) and the complexes reported by Miller and co-workers, the strength of the intrachain magnetic exchange between the Mn^{III} and TCNE$^{\bullet -}$ ions increases linearly with an increase in the dihedral angle between the mean planes of Mn^{III}(porphyrin)−TCNE$^{\bullet -}$ and Mn^{III}−N≡C. **1** showed significant magnetic anisotropy ($D_{Mn}/k_B = -3.7$ K). Furthermore, from ac susceptibility measurements, there was only one magnetic relaxation mechanism for **1** with $\Delta_\tau/k_B = 146.3$ K and $\tau_0 = 4.1 \times 10^{-10}$ s. The relaxation barrier and the significant magnetization hysteresis at low temperatures (coercive field =2.7 T at 1.8 K) are the largest yet reported for any SCM. Recent theoretical results involving SCMs beyond the Ising limit need to generalize for ferrimagnetic 1D chains. Currently, we are preparing 1D chain complexes with [Mn^{III}(TBPP)]$^+$ units linked by other organic radicals and magnetic metal ions in an effort to increase the single-ion anisotropy and exchange coupling.

ASSOCIATED CONTENT

Supporting Information

Additional structural, magnetic, spectral, and data. This material is available free of charge via the Internet at http://pubs.acs.org.

AUTHOR INFORMATION

Corresponding Author

*Tel.: +81-22-795-6548. Fax: +81-22-795-6548. E-mail: yamasita@agnus.chem.tohoku.ac.jp.

Author Contributions

All authors discussed the results and commented on the manuscript.

Notes

The authors declare no competing financial interest.

ACKNOWLEDGMENTS

This work was financially supported by a Grant-in-Aid for Scientific Research (S) (Grant No. 20225003) from the Ministry of Education, Culture, Sports, Science, and Technology, Japan.

ABBREVIATIONS

DDQ, 2,3-dichloro-5,6-dicyano-*p*-benzoquinone; TLC, thin layer chromatography, which have their usual meanings. Other abbreviations are explained in the text as well.

REFERENCES

(1) Caneschi, A.; Gatteschi, D.; Lalioti, N.; Sangregorio, C.; Sessoli, R.; Venturi, G.; Vindigni, A.; Rettori, A.; Pini, M. G.; Novak, M. A.; *Angew. Chem., Int. Ed.* 2001, *40*, 1760.

(2) Clérac, R.; Miyasaka, H.; Yamashita, M.; Coulon, C. *J. Am. Chem. Soc.* **2002**, *124*, 12837.

(3) (a) Lescouëzec, R.; Toma, L. M.; Vaissermann, J.; Verdaguer, M.; Delgado, F. S.; Ruiz-Pérez, C.; Lloret, F.; Julve, M. *Coord. Chem. Rev.* **2005**, *249*, 2691. (b) Bogani, L.; Vindigni, A.; Sessoli, R.; Gatteschi, D. *J. Mater. Chem.* **2008**, *18*, 4750. (c) Miyasaka, H.; Julve, M.; Yamashita, M.; Clérac, R. *Inorg. Chem.* **2009**, *48*, 3420. (d) Sun, H.-L; Wang, Z.-M.; Gao, S. *Coord. Chem. Rev.* **2010**, *254*, 1081. (e) Harris, T. D.; Bennett, M. V.; Clérac, R.; Long, J. R. *J. Am. Chem. Soc.* **2010**, *132*, 3980. (f) Venkatakrishnan, T. S.; Sahoo, S.; Bréfuel, N.; Duhayon, C.; Paulsen, C.; Barra, A.-L.; Ramasesha, S.; Sutter, J.-P. *J. Am. Chem. Soc.* **2010**, *132*, 6047. (g) Pardo, E.; Train, C.; Lescouëzec, R.; Journaux, Y.; Pasán, J.; Ruiz-Pérez, C.; Delgado, F. S.; Ruiz-Garcia, R.; Lloret, F.; Paulsen, Carley. *Chem. Commun.* **2010**, *46*, 2322. (h) Zhang, D.; Zhang, L.-F.; Chen, Y.; Wang, H.; Ni, Z.-H.; Wernsdorfer, W.; Jiang, J. *Chem. Commun.* **2010**, *46*, 3550. (i) Kajiwara, T.; Tanaka, H.; Nakano, M.; Takaishi, S.; Nakazawa, Y.; Yamashita, M. *Inorg. Chem.* **2010**, *49*, 8358. (j) Yang, C.-I.; Tsai, Y.-J.; Hung, S.-P.; Tsai, H.-L.; Nakano, M. *Chem. Commun.* **2010**, *46*, 5716. (k) Hoshino, N.; Sekine, Y.; Nihei, M.; Oshio, H. *Chem. Commun.* **2010**, *46*, 6117. (l) Liu, T.; Zhang, Y.-J.; Kanegawa, S.; Sato, O. *J. Am. Chem. Soc.* **2010**, *132*, 8250. (m) Zhang, S.-Y.; Shi, W.; Lan, Y.; Xu, N.; Zhao, X.-Q.; Powell, A. K.; Zhao, B.; Cheng, P.; Liao, D.-Z.; Yan., S.-P. *Chem. Commun.* **2011**, *47*, 2859. (n) Boeckmann, J.; Näther, C. *Chem. Commun.* **2011**, *47*, 7104. (o) Feng, X.; Harris, T. D.; Long, J. R. *Chem. Sci* **2011**, *2*, 1688. (p) Miyasaka, H.; Madanbashi, T.; Saitoh, A.; Motokawa, N.; Ishikawa, R.; Yamashita, M.; Bahr, S.; Wernsdorfer, W.; Clérac, R. *Chem.−Eur. J.* **2012**, *18*, 3942.

(4) Glauber, R. J. *J. Math. Phys.* **1963**, *4*, 294.

(5) (a) Coulon, C.; Clérac, R.; Lecren, L.; Wernsdorfer, W.; Miyasaka, H. *Phys. Rev. B* **2004**, *69*, 132408. (b) Wernsdorfer, W.; Clérac, R.; Coulon, C.; Lecren, L.; Miyasaka, H. *Phys. Rev. Lett.* **2005**,

95, 237−203. (c) Miyasaka, H.; Clérac, R. *Bull. Chem. Soc. Jpn.* **2005**, *78*, 1725. (d) Coulon, C.; Miyasaka, H.; Clérac, R. *Struct. Bonding (Berlin)* **2006**, *122*, 163. (e) Coulon, C.; Clérac, R.; Wernsdorfer, W.; Colin, T.; Saitoh, A.; Motokawa, N.; Miyasaka, H. *Phys. Rev. B* **2007**, *76*, 214422. (f) Coulon, C.; Clérac, R.; Wernsdorfer, W.; Colin, T.; Miyasaka, H. *Phys. Rev. Lett.* **2009**, *102*, 167−204.

(6) The Hamiltonian was defined via the following expression:

$$\mathcal{H} = -2J \sum_{-\infty}^{+\infty} S_i \cdot S_{i+1} + D \sum_{-\infty}^{+\infty} {S_{iz}}^2$$

where *S* and *D* are the ground spin state and the magnetic anisotropy parameter of the repeating unit, respectively.

(7) (a) MiyasakaH.CléracR.MizushimaK.SugiuraK.-i.YamashitaM.WernsdorferW.CoulonC.*Inorg. Chem.***2003***42*8203 (b) Saitoh, A.; Miyasaka, H.; Yamashita M.; Clérac R. *J. Mater. Chem.* **2007**, *17*, **2002**. (c) Miyasaka, H.; Saitoh, A.; Yamashita, M.; Clérac, R. *Dalton Trans.* **2008**, 2422.

(8) Ferbinteanu, M.; Miyasaka, H.; Wernsdorfer, W.; Nakata, K.; Sugiura, K.-i.; Yamashita, M.; Coulon, C.; Clérac, R. *J. Am. Chem. Soc.* **2005**, *127*, 3090.

(9) (a) Bałanda, M.; Rams, M.; Nayak, S. K.; Tomkowicz, Z.; Haase, W.; Tomala, K.; Yakhmi, J. V. *Phys. Rev. B* **2006**, *74*, 224421. (b) Vindigni, A. *Inorg. Chim. Acta* **2008**, *361*, 3731. (c) Billoni, O. V.; Pianet, V.; Pescia, D; Vindigni, A. *Phys. Rev. B* **2011**, *84*, 064415.

(10) (a) Miller, J. S.; Calabrese, J. C.; McLean, R. S.; Epstein, A. J. *Adv. Inorg. Mater* **1992**, *4*, 498. (b) Zhou, P.; Morin, B. G.; Epstein, A. J.; McLean, R. S.; Miller, J. S. *J. Appl. Phys.* **1993**, *73*, 6569. (c) Miller, J. S.; Epstein, A. J. *Angew. Chem., Int. Ed. Engl.* **1994**, *33*, 385. (d) Miller, J. S.; Vazquez, C.; Calabrese, J. C.; McLean, R. S.; Epstein, A. J. *Adv. Mater.* **1994**, *6*, 217. (e) Miller, J. S.; Vazquez, C.; Jones, N. L.; McLean, R. S.; Epstein, A. J. *J. Mater. Chem.* **1995**, *5*, 707. (f) Böhm, A.; Vazquez, C.; Mclean, R. S.; Calabrese, J. C.; Kalm, S. E.; Manson, J. L.; Epstein, A. J.; Miller, J. S. *Inorg. Chem.* **1996**, *35*, 3083. (g) Brinckerhoff, W. B.; Morin, B. G.; Brandon, E. J.; Miller, J. S.; Epstein, A. J. *J. Appl. Phys.* **1996**, *79*, 6147. (h) Gîrţu, M. A.; Wynn, C. M.; Sugiura, K.-i.; Miller, J. S.; Epstein, A. J. *J. Appl. Phys.* **1997**, *81*, 4410. (i) Griesar, K.; Athanassopoulou, M. A.; Bustamante, E. S.; Haase, W.; Tomkowicz, Z.; Zaleski, A. J. *Adv. Mater.* **1997**, *9*, 45. (j) Sugiura, K.-i.; Mikami, S.; Tanaka, T.; Sawada, M.; Manson, J. L.; Miller, J. S.; Sakata, Y. *Chem. Lett.* **1997**, 1071. (k) Brandon, E. J.; Arif, A. M.; Burkhart, B. M.; Miller, J. S. *Inorg. Chem.* **1998**, *37*, 2792. (l) Brandon, E. J.; Rittenberg, D. K.; Arif, A. M.; Miller, J. S. *Inorg. Chem.* **1998**, *37*, 3376. (m) Brandon, E. J.; Kollmar, C.; Miller, J. S. *J. Am. Chem. Soc.* **1998**, *120*, 1822. (n) Miller, J. S.; Epstein, A. J. *Chem. Commun.* **1998**, 1319. (o) Rittenberg, D. K.; Miller, J. S. *Inorg. Chem.* **1999**, *38*, 4838. (p) Rittenberg, D. K.; Sugiura, K.-i.; Sakata, Y.; Guzei, I. A.; Rheingold, A. L.; Miller, J. S. *Chem.−Eur. J.* **1999**, *5*, 1874. (q) Rittenberg, D. K.; Arif, A. M.; Miller, J. S. *J. Chem. Soc., Dalton Trans.* **2000**, 3939. (r) Miller, J. S. *Inorg. Chem.* **2000**, *39*, 4393. (s) Rittenberg, D. K.; Baars-Hibbe, L.; Böhm, A.; Miller, J. S. *J. Mater. Chem.* **2000**, *10*, 241. (t) Sugiura, K.-i.; Ushiroda, K.; Johnson, M. T.; Miller, J. S.; Sakata, Y. *J. Mater. Chem.* **2000**, *10*, 2507. (u) Hibbs, W.; Rittenberg, D. K.; Sugiura, K.-i.; Burkhart, B. M.; Morin, B. G.; Arif, A. M.; Liable-Sands, L.; Rheingold, A. L.; Sundaralingam, M.; Epstein, A. J.; Miller, J. S. *Inorg. Chem.* **2001**, *40*, 1915. (v) Fardis, M.; Diamantopoulos, G.; Papavassiliou, G.; Pokhodnya, K.; Miller, J. S.; Rittenberg, D. K.; Christides, C. *Phys. Rev. B* **2002**, *66*, 064422. (w) Etzkorn, S. J.; Hibbs, W.; Miller, J. S.; Epstein, A. J. *Phys. Rev. Lett.* **2002**, *89*, 207201. (x) Etzkorn, S. J.; Hibbs, W.; Miller, J. S.; Epstein, A. J. *Phys. Rev. B* **2004**, *70*, 134419. (y) Ribas-Ariño, J.; Novoa, J. J.; Miller, J. S. *J. Mater. Chem.* **2006**, *16*, 2600. (z) Her, J.-H.; Stephens, P. W.; Bagnato, J. D.; Miller, J. S. *J. Phys. Chem. C* **2010**, *114*, 20614.

(11) (a) Wynn, C. M.; Gîrţu, M. A.; Miller, J. S.; Epstein, A. J. *Phys. Rev. B* **1997**, *56*, 315. (b) Wynn, C. M.; Gîrţu, M. A.; Miller, J. S.; Epstein, A. J. *Phys. Rev. B* **1997**, *56*, 14050. (c) Wynn, C. M.; Gîrţu, M. A.; Brinckhoff, W. B.; Sugiura, K.-i.; Miller, J. S.; Epstein, A. J. *Chem. Mater.* **1997**, *9*, 2156. (d) Brandon, E. J.; Rogers, R. D.; Burkhart, B. M.; Miller, J. S. *Chem.−Eur. J* **1998**, *4*, 1938. (e) Johnson, M. T.; Arif, A. M.; Miller, J. S. *Eur. J. Inorg. Chem.* **2000**, *6*, 1781. (f) Sugiura, K.-i.; Mikami, S.; Johnson, M. T.; Miller, J. S.; Iwasaki, K.; Umishita, K.; Hino, S.; Sakata, Y. *J. Mater. Chem.* **2000**, *10*, 959. (g) Sugiura, K.-i.; Mikami, S.; James, M. T.; Raebiger, J. W.; Iwasaki, K.; Miller, J. S.; Okada, Y.; Hino, S.; Sakata, Y. *J. Mater. Chem* **2001**, *11*, 2152. (h) Dawe, L. N.; Miglioi, J.; Turnbow, L.; Taliaferro, M. L.; Shum, W. W.; Bagnato, J. D.; Zakharov, L. N.; Rheingold, A. L.; Arif, A. M.; Fourmigué, M.; Miller, J. S. *Inorg. Chem.* **2005**, *44*, 7530.

(12) Johnstone, R. A. W.; Nunes, M. L. P. G.; Pereira, M. M.; d'A Rocha Gonsalves, A. M.; Serra, A. C. *Heterocycles* **1996**, *43*, 1423.

(13) Kahn, O., *Molecular Magnetism*; VCH: Weinheim, Germany, 1993; Chapter 10.

(14) CrystalStructure 3.8.2: Crystal Structure Analysis Package; Rigaku Corporation (2000−2006), Tokyo, Japan.

(15) SIR97: Altomare, A.; Burla, M. C.; Camalli, M.; Cascarano, G. L.; Giacovazzo, C.; Guagliardi, A.; Moliterni, A. G. G.; Polidori, G.; Spagna, R. *J. Appl. Crystallogr.* **1999**, *32*, 115−119.

(16) SHELXL: Sheldrick, G. M. *Acta Crystallogr., Sect. A: Found. Crystallogr.*. **2008**, *A64*, 112−122.

(17) Sugiura, K.-i.; Mikami, S.; Tanaka, T.; Sawada, M.; Sakata, Y. *Chem. Lett.* **1998**, 103.

(18) (a) Hathaway, B. J. *Struct. Bonding (Berlin)* **1973**, *14*, 49. (b) Addison, A. W.; Nageswara, T.; Reedijk, J.; van Rijn, J.; Verchoor, G. C. *J. Chem. Soc., Dalton Trans.* **1984**, 1349.

(19) (a) Behere, D. V.; Mitra, S. *Inorg. Chem.* **1980**, *19*, 992. (b) Behere, D. V.; Marathe, V. R.; Mitra, S. *Chem. Phys. Lett.* **1981**, *81*, 57. (c) Dugad, L. B.; Behere, D. V.; Marathe, V. R.; Mitra, S. *Chem. Phys. Lett.* **1984**, *104*, 353. (d) Kennedy, B. J.; Murray, K. S. *Inorg. Chem.* **1985**, *24*, 1557. (e) Goldberg, D. P.; Telser, J.; Krzystek, J.; Montalban, A. G.; Brunel, L.-C.; Barrett, A. G. M.; Hoffman, B. M. *J. Am. Chem. Soc.* **1997**, *119*, 8722. (f) Yates, M. L.; Arif, A. M.; Manson, J. L.; Kalm, B. A.; Burkhart, B. M.; Miller, J. S. *Inorg. Chem.* **1998**, *37*, 840. (g) Krzystek, J.; Telser, J. *J. Magn. Reson.* **2003**, *162*, 454. (h) Harvey, J. D.; Ziegler, C. J.; Telser, J.; Ozarowski, A.; Krzystek, J. *Inorg. Chem.* **2005**, *44*, 4451. (i) Horitani, M.; Yashiro, H.; Hagiwara, M.; Hori, H. *J. Inorg. Biochem* **2008**, *102*, 781.

(20) (a) Summerville, D. A.; Cape, T. W.; Johnson, E. D.; Basolo, F. *Inorg. Chem.* **1978**, *17*, 3297. (b) Jones, R. D.; Summerville, D. A.; Basolo, F. *J. Am. Chem. Soc.* **1978**, *100*, 4416.

(21) (a) Khatkale, M. S.; Devlin, J. P. *J. Phys. Chem.* **1979**, *83*, 1636. (b) Miller, J. S. *Angew. Chem., Int. Ed.* **2006**, *45*, 2508.

(22) Seiden, J. *J. Phys., Lett.* **1983**, *44*, L947.

(23) (a) Loveluck, J. M.; Lovesey, S. W.; Aubry, S. *J. Phys. C: Solid State Phys.* **1975**, *8*, 3841. (b) Nakamura, K.; Sasada, T. *J. Phys. C: Solid State Phys.* **1978**, *11*, 331.

(24) Mydosh, J. A. *Spin Glasses: An Experimental Introduction*; Taylor & Francis: London, 1993.

(25) (a) Cole, K. S.; Cole, R. H. *J. Chem. Phys.* **1941**, *9*, 341. (b) Boettcher, C. J. F. *Theory of Electric Polarisation*; Elsevier: Amsterdam, 1952. (c) Aubin, S. M.; Sun, Z.; Pardi, L.; Krzysteck, J.; Folting, K.; Brunel, L.-J.; Rheingold, A. L.; Christou, G.; Hendrickson, D. N. *Inorg. Chem.* **1999**, *38*, 5329.

(26) de Jongh, L. J.; Miedema, A. R. *Adv. Phys.* **1974**, *23*, 1.

(27) Miyasaka, H.; Madanbashi, T.; Sugimoto, K.; Nakazawa, Y.; Wernsdorfer, W.; Sugiura, K.-i.; Yamashita, M.; Coulon, C.; Clérac, R. *Chem.−Eur. J.* **2006**, *12*, 7028.

(28) Bałanda, M.; Tomkowicz, Z.; Haase, W.; Rams, M. *J. Phys. Conf. Ser.* **2011**, *303*, 012036.